ARTICLE

ACS chemical biology

Light-Activated Gene Expression Directs Segregation of Co-cultured Cells *in Vitro*

Daniel J. Sauers, Murali K. Temburni[†], John B. Biggins, Luke M. Ceo, Deni S. Galileo, and John T. Koh*

Departments of Chemistry and Biochemistry and Biological Sciences, University of Delaware, Newark, Delaware 19716, [†]Current address: Department of Biology, Georgian Court University, Lakewood, NJ 08701.

ABSTRACT Light-directed gene patterning methods have been described as a means to regulate gene expression in a spatially and temporally controlled manner. Several methods have been reported that use photocaged forms of small molecule effectors to control ligand-dependent transcription factors. Whereas these methods offer many advantages including high specificity and transient light-sensitivity, the free diffusion of the uncaged effector can limit both the magnitude and resolution of localized gene induction. Methods to date have been limited by the small fraction of irradiated cells that have expression levels significantly above uninduced background and have not been shown to affect a defined biological response. The tetracycline-dependent transactivator/transrepressor system, RetroTET-ART, combined with a photocaged form of doxycycline (NvOC-Dox) can be used to form photolithographic patterns of induced expression wherein up to 85% of the patterned cells show expression levels above uninduced regions. The efficiency and inducibility of the RetroTET-ART system allows one to quantitatively measure the limits of resolution and the relative induction levels mediated by a small molecule photocaged effector for the first time. Well-defined patterns of reporter genes were reproducibly formed within 6−36 h with feature sizes as small as 300 μm. After photo-patterning, NvOC-Dox can be rapidly removed, rendering cells photoinsensitive and allowing one to monitor GFP product formation in real time. Patterned co-expression of the cell surface ligand ephrin A5 on cell monolayers creates well-defined patterns that are sufficient to direct and segregate co-cultured cells *via* either attractive or repulsive signaling cues. The ability to direct the arrangement of cells on living cell monolayers through the action of light may serve as a model system for engineering artificial tissues.

Precise spatial and temporal control of gene expression is essential to the organization of complex tissues, including pattern formation during tissue development (*1, 2*). The study of guidance cues and other forms of intercellular communication that rely on the coordinated expression of genes in multicellular patterns can be hindered by the limited methods available to precisely control patterned gene expression *in vivo* or *in vitro*. Recreating such phenomenon in *in vitro* cell culture can provide important validation in controlled systems for the roles of various attractive and repulsive cues in normal development and cancer. The precise spatial and temporal control of expression of cell signaling molecules *in vitro* can serve as the basis for creating more advanced artificial tissues *in vitro*. Several methods have been developed to control spatiotemporal gene expression by placing genes of interest under the control of light using photocaged molecules that regulate gene expression only when converted into a biologically active form though the action of light (*3–13*). Many of these systems utilize photocaged biopolymers that are generally difficult to deliver into cells and are typically introduced by microinjection into oocytes, resulting in an organism that subsequently remains light-sensitive (*3, 5, 14–16*). Photocaged ligands of nuclear hormone receptors or ligand-dependent repressors/activators readily enter cells and render systems photosensitive only upon treatment with caged effectors (*4, 6, 17–22*). However, once uncaged, small molecule ligands can readily diffuse away from the site of uncaging, potentially limiting the efficiency and magnitude of response, which limits the spatial resolution of the induced pattern of protein expression (*19*). Recent reports of light-directed gene patterning by small molecule effectors show that only a small fraction of the irradiated cells have expression levels significantly above

*Corresponding author, johnkoh@udel.edu.

Received for review September 21, 2009 and accepted January 5, 2010.

Published online January 5, 2010

10.1021/cb9002305

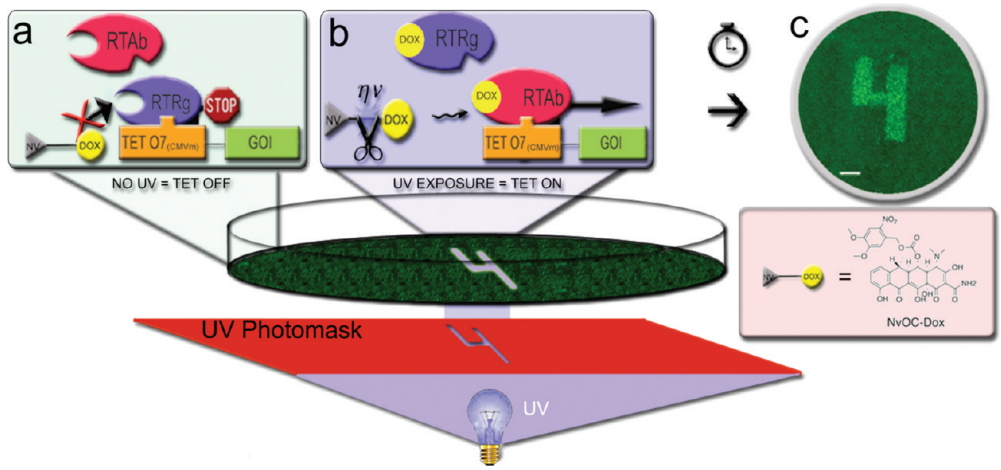

Figure 1. Light-directed gene patterning with photomasks using Retro TET-ART. a) Near-confluent monolayers of 3T3 cells with gene of interest (GFP) under control of the Retro-Tet ART system. The transrepressor remains bound in the presence of NvOC-Dox. b) A photomask is used to selectively irradiate cells in a desired pattern. Liberated dox causes the release of the transrepressor and recruitment of the transactivator to the Tet operator. c) An actual pattern of induced gene expression corresponding to the shape of the photomask (scale bar = 1 mm).

uninduced background levels, which can significantly limit potential applications (*8, 23*). Herein we report the first efficient gene patterning system that enables one to generate well-defined photolithographic patterns, to evaluate quantitatively the spatial resolution and the time course of photoactivated gene expression, and demonstrate the physiological relevance of such patterns by directing co-cultured cells through attractive and repulsive cues.

RESULTS AND DISCUSSION

The first reported examples of light-activated gene expression by small molecule effectors used caged agonists of nuclear/steroid hormone receptors (*4, 6*). After surveying the estrogen receptor, thyroid hormone receptor, and ecdysone receptor based systems (*24*), some of which lacked efficiency and quick inducibility in *in vitro* confluent cell monolayers, we found that in our hands the tetracycline based RetroTET-ART (*25*) system provided a robust response to transient ligand exposure intrinsic to localized activation by effectors that can diffuse from the site of uncaging. Contact-inhibited cells (NIH 3T3) that stop dividing once confluent to form well-defined monolayers were selected for patterning experiments as they form stable patterned monolayers appropriate for studying intercellular interactions of co-cultured cells *in vitro*.

Stable 3T3 cell lines that express tet-inducible GFP (HRSp-GFP) under the control of the RetroTET-ART system were created by multiple rounds of infection, selection, and FACS sorting (*25*). Application of photocaged doxycyline (nitroveratryloxydoxycycline, Nv-Dox) has been described recently as a regulator of "Tet-on" dependent transcription (*18*). Using the tet transactivator RTAb alone, less than 30% of confluent 3T3 cells are activated above uninduced levels upon treatment for 2 h with Dox. By contrast, the full RetroTET-ART system, which employs both a tetracycline (tet) dependent transrepressor (tTRg) and a retro-tet transactivator (rtRAb), was found to activate greater than 90% of cells above uninduced levels under the same conditions (see Supporting Information). We have prepared a photocaged form of doxycycline (nitroveratryloxycarbonyl doxycycline, or NvOC-Dox). Preparations of NvOC-Dox show no increase in background GFP expression up to 29 μM. Brief UVA exposure of cells containing 6 μM NvOC-Dox resulted in levels of GFP expression comparable to direct treatment with 9 μM dox for 2 h. No change in fluorescence was observed after equivalent irradiation in the absence of the caged ligand (see Supporting Information).

Time-Dependence of Light-Activated GFP Patterning. Spatially confined patterns of UVA (330−380 nm) irradiation were generated using photomasks of UV-absorbing polyester filters placed directly on the bot-

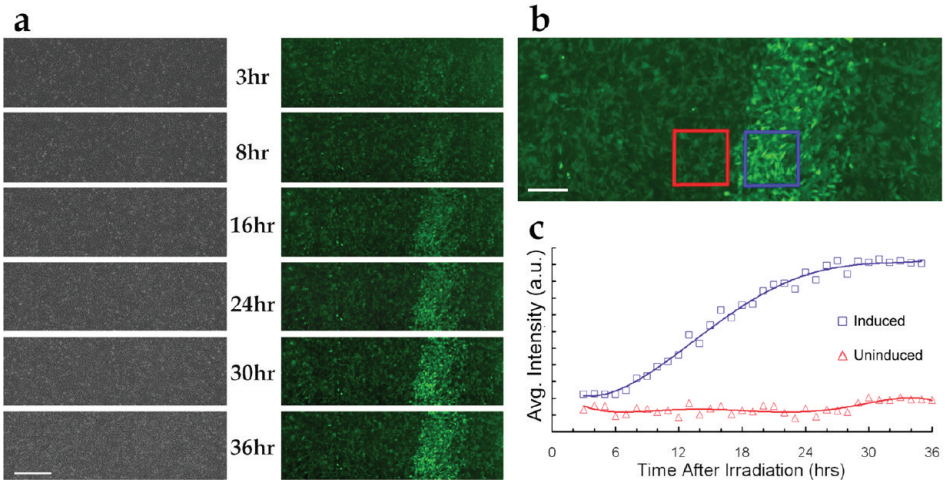

Figure 2. a) Time lapse images of light-directed gene patterning of GFP. A near confluent monolayer of HRSp-GFP 3T3 cells was treated with 6 μM NvOC-Dox and irradiated for a total of 120 s with UVA light through a 344 μm photomask. Time-lapse images acquired over 36 h showed the emergence of a pattern of GFP expression in the region of irradiation (right), while the phase contrast images (left) show no change in cell morphology due to the UVA exposure (scale bar = 500 μm). b) The induced and uninduced regions of the pattern used to calculate the average relative increase in GFP fluorescence (red = uninduced, blue = induced) (scale bar = 250 μm). c) Time-dependent induction of relative fluorescence in induced versus uninduced regions relative to untransfected 3T3 cells approached 5-fold in 26 h.

tom of tissue culture dishes using a Nikon TE-2000E equipped with a 100 W Hg-Arc lamp through a Nikon 4X objective using a Nikon UV-1 filter (see Supporting Information). HRSP-GFP 3T3 cells were grown to near confluence and treated with media containing 6 μM of NvOC-Dox 30 min prior to irradiation through the photomask (Figure 1). After irradiation, the media was exchanged with ligand-free media. No longer light-responsive, the cells could be monitored using both brightfield and fluorescence imaging without altering the pattern of GFP expression (see Supporting Information). To obtain increased sensitivity and higher resolution, composite images (40−60 megapixel) were compiled by tiling a series of high magnification images.

Time-lapse images taken over 36 h showed the emergence of a clearly differentiated pattern of GFP expression at 4−6 h and approached a maximum intensity after 26 h (Figure 2, panel a). Photorelease of doxycycline is many orders of magnitude faster than the process of transcription/translation and the relatively slow formation of the GFP chromophore (*26*). Thus the time-dependent induction of observed GFP fluorescence is similar to that previously reported after adding doxycycline to HRSP-GFP-expressing cells (*25*). No morphological changes could be seen as the result of the UV exposure in the phase contrast images (Figure 2, panel a, left). Using a photomask that was 244 μm in width, a patterned stripe of GFP expression roughly 570 μm began to appear as early as 4−6 hours and approached a maximum after 26 hours (Figure 2, panel a, right and Supporting Information). Patterns made in this manner were still visible 4 days after irradiation. Under the described experimental conditions, 70−85% of the cells within the photoexposed region were clearly induced above background, allowing us to clearly define the boundaries of the patterned response and measure the relative induction of patterned response. Relative induction of GFP expression was determined by comparing the average fluorescence intensity of induced and uninduced regions of the pattern that are separated by only 65 μm (Figure 2, panel c). The time-dependent expression profile shows that the relative level of GFP expression was 4.9-fold higher in the patterned area than in the unirradiated areas, which remained essentially unchanged. Despite the transient exposure to uncaged doxycycline, this represents approximately 50% of the induction observed when similar cells were treated with 9 μM of dox for 2 h. Using contact-inhibited cell monolayers and photomasks, we have been able to achieve

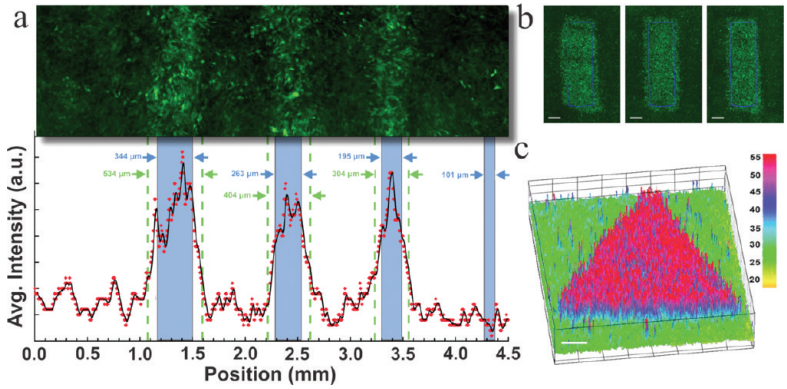

Figure 3. Resolution, reproducibility, and intensity of photoinduced patterns of GFP expression. a) The limits of resolution of photoinduced patterns of gene expression using a photomask of decreasing line widths (shown in blue) and the resulting patterns of expression shown as a line scan (average vertical) intensity profile. The smallest reproducible pattern was a 304 μm wide stripe from a 195 μm wide template. b) Nearly identical images can be reliably reproduced using the same photomask (scale bar = 500 μm). With a photomask template of 970 μm × 3404 μm, the resulting patterns were, left = 1275 μm × 3775 μm, middle = 1340 μm × 3720 μm, and right = 1230 μm × 3700 μm. c) A 3D surface plot of intensity for a patterned triangle of GFP expression about 4 mm per side that shows the relative induction with 8-bit image intensity values (scale bar = 500 μm).

highly induced and resolved patterns of gene expression that were sustained for many days.

Light-activated gene patterning using small molecule effectors can provide resolved patterns of inducible gene expression *in vitro*. The caged effector NvOC-Dox diffuses readily in and out of cells to render cellular systems transiently light-sensitive. After local uncaging, the small molecule ligand diffuses away from the patterned region, limiting the duration and potentially the intensity of gene response. For tightly binding ligand–receptor complexes, the duration of transcription response is much longer due to the slow off-rate of the ligand from the ligand–receptor complex and the half-life of the reporter protein GFP. In our studies, light-induced GFP expression continued to rise up to 26 h after photopatterning, long after effective concentrations of free ligand are lost to diffusion.

Pattern Reproducibility and Resolution. The NvOC-Dox/RetroTet-ART system was capable of creating patterns of many shapes and sizes. In all cases, the photoirradiated regions, though clearly visible by fluorescence (GFP) imaging, were indiscernible by phase contrast imaging. As an additional assay of induced gene expression, patterned cell cultures were immunostained with anti-GFP antibodies. The resulting immunofluorescence images matched the regions observed by direct GFP fluorescence, thus supporting that the GFP fluorescence images were the result of an increase in GFP expression and not from alteration of the inherent fluorescent properties of the irradiated cells (see Supporting Information).

The high percentage of responsive cells observed by this method allows one to form patterns with well-defined boundaries and to test the limits of resolution attainable by a soluble effector. Whereas regions of induced expression were obtained in every experiment, sharp patterns closely matching that of the photomask were obtained only 20–30% of the time. Distorted or more poorly defined patterns having regions of low induction were observed in the remaining cases (see Supporting Information). Pattern distortion can be caused by inadvertently disturbing the culture just after irradiation. Regions of poor induction or irregularly shaped patterns are circumstantially linked to uneven cell plating (*i.e.*, local degree of confluency) of the cell monolayer; confluent cells appear to be less responsive to transient exposure to uncaged ligand. Within these limitations, the same photomask could be used to reproduce nearly identical patterns multiple times (Figure 3, panel b).

The feature sizes that can be created by methods that employ small molecule effectors are limited by ligand diffusion, which requires a balance between generating a sufficiently high local concentration of effector to trigger a transcriptional response while limiting the amount of effector that diffuses into adjacent regions of cells. The lower limit of feature sizes that can be patterned by this system may be approximated using a photomask composed of multiple stripes of decreasing widths. A 195 μm wide photomasked stripe formed a 304 μm strip of GFP-expressing cells, and although a photomask strip of 101 μm did provide some cells with clearly induced expression, induction was inconsistent and failed to form a well-defined pattern (Figure 3, panel a). The pattern of induced gene expression was always larger than the size of the photomask, due in part to optical diffraction and the diffusion of uncaged doxycycline into adjacent cells. The larger size of the GFP-expressing cells does not appear to be due to cell migration as time lapse image analysis shows that cell migrate on average only 13 ± 9 μm over the experiment in these contact-inhibited cell monolayers. The

photomask method can create patterns to the resolution limits of the NvDox/RetroTet-ART system, is operationally simple, and can be adapted to any common laboratory microscope.

Ligand diffusion does limit pattern resolution. Whereas sufficient uncaged ligand is formed to create patterns with 50% of the maximum inducible expression, narrow features do not give rise to significant expression, presumably because the uncaged ligand is more rapidly diluted through diffusion. Although it is possible to obtain patterns from smaller features using a higher initial concentration of ligand, this might also cause gene activation in neighboring regions to increase. Ultimately, the resolution of the patterns that can be achieved may depend on the efficiency of ligand caging, which limits the concentration of caged ligand that can be used as well as the diffusion rate of the ligand out of the cell and its on/off rates with the receptor.

Multigene Patterning and Segregation of Cocultured Cells. Whereas differences in fluorescence intensity between on and off pattern regions of cell monolayer are easily discernible by imaging, it remains to be demonstrated if these differences in light-directed gene expression are sufficient to cause a physiologically relevant effect. An important application of light-activated gene expression can be to direct multicellular organization to form artificial tissues. The membrane-bound ephrin ligands and their Eph tyrosine kinase receptors help mediate cell−cell interactions of many different developmental processes (*27–29*). While the interaction between the EphA7 receptor and the ligand ephrin A5 generally mediates a repulsive signal between cells (*30–32*), the naturally occurring splice variant, EphA7-T1, which lacks its tyrosine kinase signaling domain (*33*), provides attractive interactions with ephrin A5 that aid in the proper fusion of cranial neural folds at the dorsal midline during mouse brain development (*34, 35*). The opposing effects of EphA7 variants toward ephrin A5-expressing cells can be used to direct cells toward or away from regions of induced ephrin A5 expression.

A new 3T3 cell line was created that provides tet inducible expression of ephrin A5 under control of the RetroTet ART transrepressor/retrotransactivator. In order to directly visualize the regions of ephrin expression in real time, the ephrin A5 cDNA was subcloned downstream of GFP in HRSp-GFP linked in-frame *via* the aphthovirus 2A polyprotein sequence. The 2A sequence is a short amino acid sequence containing a terminal P-G-P that leads to intraribosomal cleavage of the nascent polypeptide before the terminal proline, thus providing an efficient means of making multicistronic vectors that result in a 1:1 expression of multiple proteins (*36–38*). In response to Tet, the HRSp-GFP-2A-ephrinA5 vector provides equimolar production of GFP that is coincidental with ephrin A5 (Figure 4 and Supporting Information).

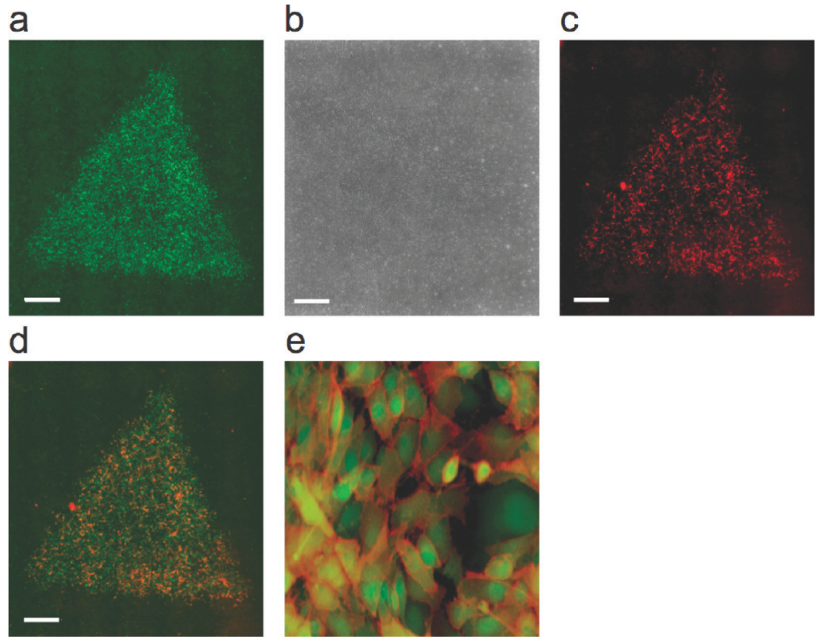

Figure 4. Coincidental expression of GFP and ephrin A5 expression using the aphthovirus 2A polyprotein cleavage sequence. a) Pattern of increased ephrin A5 expression, visualized by GFP fluorescence and b) the phase image of the same cells. c) The pattern was stained with an antiephrin A5 antibody. d) The resulting red pattern is nearly identical to that of the GFP as seen in an image overlay. e) Enlargement of image d confirms proper 2A cleavage, with surface staining of the ephrin A5 and cytoplamic GFP. All scale bars = 500 μm.

Cell monolayers expressing spatially discrete photopatterned ephrin A5/GFP were evaluated for their ability to direct adhesion of HEK293T cells expressing full length or truncated forms of the EphA7 receptor. EphA7-T1-expressing 293T cells preferentially adhere to the regions of the 3T3 monolayers expressing induced ephrin A5 (Figure 5, panels a−c). Under identical conditions, no adhesion is observed when EphA7-T1-expressing 293T cells are added to untransfected 3T3 monolayers. The selective adhesion of the 293T

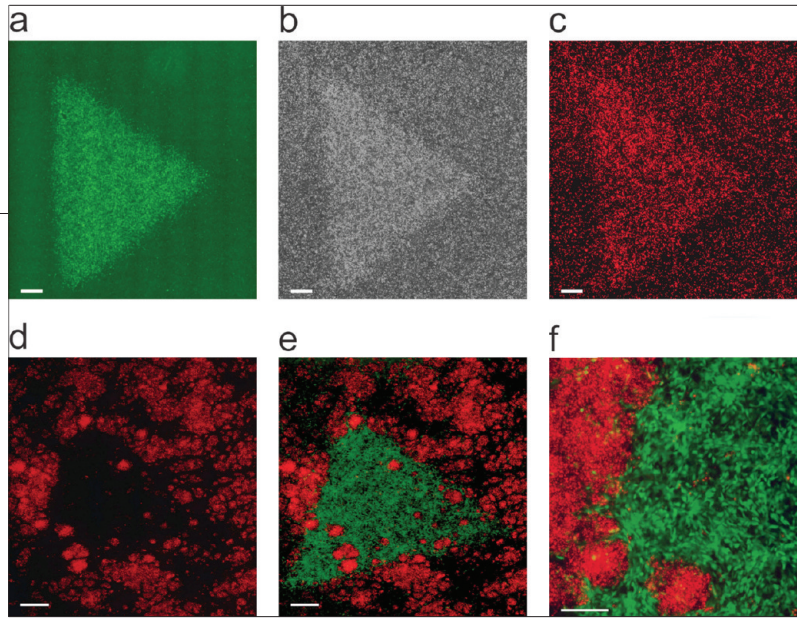

Figure 5. Segregation of EphA7-T1-expressing (a−c) and EphA7-expressing (d−f) 293T cells by cell monolayers with patterned ephrin A5/GFP expression. a) Pattern of induced ephrin A5 expression visualized by co-translated GFP fluorescence. b) Phase contrast image of EphA7-T1-expressing 293T cells adhering to a 3T3 monolayer with patterned ephrin A5 expression. c) Fluorescence image of DiI-labeled EphA7-T1-expressing 293T cells, showing preferential adhesion to the region of induced ephrin A5. d) DiI-labeled EphA7-expressing 293T cells co-cultured for 48 h on ephrin A7 patterned 3T3 monolayers. e) EphA7 293T cells (red) merged with pattern of ephrin A5 expression visualized by co-translated GFP. f) Higher magnification of boundary region. Scale bars for a, b, and c = 500 μm. Scale bar for d = 250 μm.

cells to the region of patterned ephrin A5/GFP expression was directly visible in the phase contrast images (Figure 5, panel a). Fluorescence image analysis of the fluorescent vital dye (DiI)-labeled EphA7-T1-expressing 293T cells combined with the co-translated expression of GFP allows one to monitor the pattern and the co-cultured cells in real time. The attractive interactions between ephrin A5 patterned on the monolayer and the full length EphA7 expressed in the labled co-cultured 293T cells provided a well-defined pattern representing a 97% increase in 293T cells in the regions of ephrin A5 expression measured by the increase in integrated fluorescence intensity (Figure 5, panel c and Supporting Information).

Cells expressing the full length EphA7 were also created, labeled with DiI and co-cultured with 3T3 cell monolayers expressing freshly patterned ephrin A5 (Figure 5, panels d−f). In contrast to cells expressing the truncated EphA7-T1, cells expressing full-length EphA7 were repelled by the regions of photoinduced ephrin A5 expression and were found 3.1-fold less frequently in the triangular patterned region than outside the region (Figure 4, panel e). Note, however, that in a few spots, EphA7-expressing 293T cells were able to invade regions of patterned ephrin A5 to form well segregated clusters, a phenomenon presumably created by cells adhering to the substrate through gaps in the monolayer that grew to displace the monolayer (Figure 5, panels and f). Excluding these well-defined localized clusters, the density of EphA7-expressing cells was 105-times lower in the patterned region than in the adjacent nonpatterned region (Supporting Information). Together these studies demonstrate that multigene patterned monolayers can be used to segregate and direct co-cultured cells using both attractive and repulsive guidance cues *in vitro*, providing a means to control the arrangement of cells in three dimensions. Such systems form the basis for creating complex artificial tissues *in vitro* and provide new tools for studying phenomena such as differentiation and development that are dependent on coordinated expression of genes in multicellular patterns.

METHODS

Plasmid Description and Cell Line Creation. HRSP-GFP-2A-ephrin A5 was created by amplifying the ephrin A5 gene with a forward primer containing a 2A sequence (gag ggc cgc ggc tcc ctc ctc acc tgc ggc gac gtc gag gag aac ccc ggc ccc or E G R G S L L T C G D V E E N P G P) in frame. This fragment was ligated into the AgeI and ClaI sites of HRSpuro-GFP (*36–38*). A Western blot confirmed that the proper transcriptional cleavage was occurring at the 2A sequence, and immunostaining supported the surface expression of ephrin A5 with intracellular expression of GFP see (Supporting Information). Both HRSp-GFP amd HRSP-GFP-2A-ephrin A5 plasmids were used to create stable NIH 3T3 cell lines using the calcium phosphate method. Doxycycline-inducible cell lines were created for each by viral infection with the transactivator (RTAb) and transrepressor (RTRg) of the RetroTet-ART inducible system as previously described (*36–38*).

Synthesis and Purification of NvOC-Dox. To a solution of doxycycline hyclate (150 mg, 0.29 mmol) and 4 Å molecular sieves in anhydrous methylene chloride (1.5 mL) at 0 °C was added diisopropylethyl amine (52.3 μL, 0.61 mmol). After 5 min, a solution of nitroveratryl chloroformate (80.75 mg, 0.29 mmol) in anhydrous dichloromethane (1.5 mL) was added *via* canula. The reaction mixture was allowed to gradually warm to RT and was stirred for 15 h. The crude mixture was chromatographed on silica gel using a gradient (0−5%) of methanol in dichloromethane to afford 33.7 mg (0.049 mmol, 17%) of NvOC-Dox. ^{1}H NMR (DMSO-d_6, 600 MHz, δ): 1.52 (d, J = 6.70 Hz, 3H, 6MeH), 2.43 (s, 6H, C-4 N(CH_3)$_2$), 2.56 (m, 1H, 5aH), 2.84 (m, 1H, 6H), 3.85 (s, 3H, 8′′MeH), 3.95 (s, 3H, 7′′MeH), 4.24 (br s, 1H, 4a), 5.46 (d, J = 14.6 Hz, 1H, 1′′aH), 5.57 (d, J = 14.5 Hz, 1H, 1′′bH), 6.84 (d, J = 8.2 Hz, 1H, 9H), 6.95 (d, J = 8.0 Hz, 1H, 7H), 7.16 (s, 1H, 6′′H), 7.51 (t, J = 8.1 Hz, 1H, 8H), 7.70 (s, 1H, 9′′H), 9.12 (br s, 2H, C-2 $CONH_2$), 11.65 (br s, 1H, C-10 OH), 14.97 (br s, 1H, OH). ^{13}C NMR (DMSO-d_6, 400 MHz, δ): 194.5, 192.9, 183.2, 174.19, 173.18, 161.40, 153.51, 148.21, 147.86, 138.90, 138.64, 134.18, 127.09, 117.5, 116.56, 115.74, 111.74, 108.27, 107.8, 91.5, 72.38, 68.11, 65.92, 65.61, 56.28, 55.98,

48.60, 45.40, 42.28, 38.52, 38.12, 37.10, 16.16. HRMS (ESI) [M+1] calcd for $C_{32}H_{34}N_3O_{14}$ 684.20400; found 684.20400.

Photoinduced Patterning Procedure. 3T3 cells were seeded into individual 60 mm plastic dishes (Falcon) such that they would form a nearly confluent monolayer in 48 h. Successful photo-patterning was obtained when the monolayer was closely and evenly spaced, while maintaining a "spiky" appearance (see Supporting Information). Under red light conditions, media containing the appropriate amount of NvOC-Dox (up to 6 μM for HRSp-GFP and up to 18 μM for HRSp-GFP-2A-ephrin A5) was added to the cells and allowed to incubate for 30 min prior to irradiation. Photomasks were made using Roscolux polyester color gel no. 27 (medium red), due to its 0% transmittance of light above 400 nm (400−600 nm) (see Supporting Information). The desired photomask was then fixed to the bottom of the cell plate and irradiated using a 100 W Hg-Arc lamp through a Nikon 4X objective using a Nikon UV-1 filter (excitation 330−380 nm), in a Nikon TE-2000E epifluorescene microscope. The duration of irradiation varied from a low of two 30 s exposures, separated by 4 min, to a high of two 120 s exposures. Whereas expression patterns created using the shortest irradiation time were sometimes visible, the majority of cells in the patterned area remained uninduced. The expression patterns with the highest percentage of induced cells within the targeted region (>90%) were created using the longest exposure time of 4 min. The position of the photomask relative to the cells was obtained from the *x* and *y* coordinates from the programmable microscope stage (Prior Proscan II). After irradiation,the cells were washed 3 times with fresh medium and the patterns typically imaged ≥20 h later.

Image Preparation and Analysis. All images were acquired using an automated time-lapse microscopy system composed of a Nikon TE-2000E epifluorescence microscope equipped with a Prior Proscan II motorized stage and controller, a 100 W Hg-Arc lamp, and a Photometrics CoolSNAP ES CCD camera using Metamorph software, which is described in detail in Fotos *et al.* (*39*) The filters used were a Nikon UV-1 for UV irradiation, a Nikon EN GFP HQ for GFP excitation, and a Nikon G-1B for red fluorescent imaging. In order to maximize sensitivity and resolution, multiple individual images taken using the 10X objective were tiled together into a single composite image. The benefits of tiling multiple images together were improved cellular resolution, a higher dynamic range of GFP intensity levels on the images, and the ability to visualize larger induced patterns of expression (up to 6 mm). The process of tiling together the numerous individual images into a single larger image was efficiently accomplished using a number of custom-made actions for Adobe Photoshop CS2 (see Supporting Information). The phase images taken at each position were used to align individual positions. The fluorescence images were then overlaid on top of the phase images and merged together to create the final image of the induced pattern of expression. All adjustments in brightness and contrast were applied equally to all of the component images of the final composite tiled image, thus preserving the significance of the relative differences between uninduced and induced regions of the image.

Acknowledgment: We thank Dr. Steve Bai for assistance with 2-D NMR experiments, Professor Helen M. Blau (Stanford University) for providing RetroTet-ART system plasmids, Professor Elena Pasquale (Burnham Institute) for the ephrin A5 expression plasmid and antibodies, and Prof. Jonas Frisén (Karolinska Institute) for providing EphA7 and EphA7-T1 expression plasmids. J.B.B. is a Robert Black Fellow of the Damon Runyon Cancer Research Foundation (DRG 1852-05). This work was supported by the National Institutes of Health (NINDS R01NS049523 and NIDDK R01DK54257).

Supporting Information Available: This material is available free of charge *via* the Internet.

REFERENCES

1. Gilbert, S. F. (2006) *Developmental Biology*, 8th ed., Sinauer Associates, Inc., Sunderland, MA.
2. Lewis, J. (2008) From signals to patterns: Space, time, and mathematics in developmental biology, *Science 322*, 399–403.
3. Ando, H., Furuta, T., Tsien, R. Y., and Okamoto, H. (2001) Photomediated gene activation using caged RNA/DNA in zebrafish embryos, *Nat. Genet. 28*, 317–325.
4. Cruz, F. G., Koh, J. T., and Link, K. H. (2000) Light-activated gene expression, *J. Am. Chem. Soc. 122*, 8777–8778.
5. Haselton, F. R., Tseng, W. C., and Chang, M. S. (1997) Light activated protein expression using caged transfected plasmid i: delivery by liposomes to cultured retinal endothelium, *Invest. Ophthalmol. Visual Sci. 38*, 2082–2082.
6. Lin, W. Y., Albanese, C., Pestell, R. G., and Lawrence, D. S. (2002) Spatially discrete, light-driven protein expression, *Chem. Biol. 9*, 1347–1353.
7. Cambridge, S. B., Davis, R. L., and Minden, J. S. (1997) Drosophila mitotic domain boundaries as cell fate boundaries, *Science 277*, 825–828.
8. Cambridge, S. B., Geissler, D., Calegari, F., Anastassiadis, K., Hasan, M. T., Stewart, A. F., Huttner, W. B., Hagen, V., and Bonhoeffer, T. (2009) Doxycycline-dependent photoactivated gene expression in eukaryotic systems, *Nat. Methods 6*, 527–U86.
9. Lee, H. M., Larson, D. R., and Lawrence, D. S. (2009) Illuminating the chemistry of life: design, synthesis, and applications of "caged" and related photoresponsive compounds, *ACS Chem. Biol. 4*, 409–427.
10. Mayer, G., and Heckel, A. (2006) Biologically active molecules with a "light switch", *Angew. Chem., Int. Ed. 45*, 4900–4921.
11. Tang, X. J., and Dmochowski, I. J. (2007) Regulating gene expression with light-activated oligonucleotides, *Mol. Biosyst. 3*, 100–110.
12. Young, D. D., and Deiters, A. (2007) Photochemical control of biological processes, *Org. Biomol. Chem. 5*, 999–1005.
13. Young, D. D., Garner, R. A., Yoder, J. A., and Deiters, A. (2009) Light-activation of gene function in mammalian cells via ribozymes, *Chem. Commun.* 568–570.
14. Shestopalov, I. A., Sinha, S., and Chen, J. K. (2007) Light-controlled gene silencing in zebrafish embryos, *Nat. Chem. Biol. 3*, 650–651.
15. Young, D. D., Lusic, H., Lively, M. O., Yoder, J. A., and Deiters, A. (2008) Gene silencing in mammalian cells with light-activated antisense agents, *ChemBioChem 9*, 2937–2940.
16. Shah, S., Rangarajan, S., and Friedman, S. H. (2005) Light-activated RNA interference, *Angew. Chem., Int. Ed 44*, 1328–1332.
17. Biggins, J. B., Hashimoto, A., and Koh, J. T. (2007) Photocaged agonist for an analogue-specific form of the vitamin D receptor, *ChemBioChem 8*, 799–803.
18. Cambridge, S. B., Geissler, D., Keller, S., and Curten, B. (2006) A caged doxycycline analogue for photoactivated gene expression, *Angew. Chem., Int. Ed. 45*, 2229–2231.
19. Link, K. H., Cruz, F. G., Ye, H.-F., O'Reilly, K., Dowdell, S., and Koh, J. T. (2004) Photo-caged agonists of the nuclear receptors RARγ and TRβ provide unique time-dependent gene expression profiles for light-activated gene patterning, *Bioorg. Med. Chem. 12*, 5949–5959.
20. Link, K. H., Shi, Y. H., and Koh, J. T. (2005) Light activated recombination, *J. Am. Chem. Soc. 127*, 13088–13089.
21. Shi, Y. H., and Koh, J. T. (2004) Light-activated transcription and repression by using photocaged serms, *ChemBioChem 5*, 788–796.
22. Young, D. D., and Deiters, A. (2007) Photochemical activation of protein expression in bacterial cells, *Angew. Chem., Int. Ed. 46*, 4290–4292.

23. Lin, W., Albanese, C., Pestell, R. G., and Lawrence, D. S. (2002) Spatially discrete, light-driven protein expression, *Chem. Biol. 9*, 1347–1353.
24. Biggins, J. B., Sauers, D., Temberni, M., Koh, J. T.Unpublished results.
25. Rossi, F. M. V., Guicherit, O. M., Spicher, A., Kringstein, A. M., Fatyol, K., Blakely, B. T., and Blau, H. M. (1998) Tetracycline-regulatable factors with distinct dimerization domains allow reversible growth inhibition by p16, *Nat. Genet. 20*, 389–393.
26. Reid, B. G., and Flynn, G. C. (1997) Chromophore formation in green fluorescent protein, *Biochemistry 36*, 6786–6791.
27. Frisen, J., Holmberg, J., and Barbacid, M. (1999) Ephrins and their Eph receptors: Multitalented directors of embryonic development, *EMBO J. 18*, 5159–5165.
28. Frisen, J., Yates, P. A., McLaughlin, T., Friedman, G. C., O'Leary, D. D. M., and Barbacid, M. (1998) Ephrin-A5 (AL-1/RAGS) is essential for proper retinal axon guidance and topographic mapping in the mammalian visual system, *Neuron 20*, 235–243.
29. Holder, N., and Klein, R. (1999) Eph receptors and ephrins: Effectors of morphogenesis, *Development 126*, 2033–2044.
30. Castellani, V., Yue, Y., Gao, P. P., Zhou, R., and Bolz, J. (1998) Dual action of a ligand for Eph receptor tyrosine kinases on specific populations of axons during the development of cortical circuits, *J. Neurosci. 18*, 4663–4672.
31. Davy, A., Gale, N. W., Murray, E. W., Klinghoffer, R. A., Soriano, P., and Feuerstein, C. (1999) Compartmentalized signaling by GPI-anchored ephrin-A5 requires the fyn tyrosine kinase to regulate cellular adhesion, *Genes Dev. 13*, 3125–3135.
32. Pandey, A., Shao, H., Marks, R. M., Polverini, P. J., and Dixit, V. M. (1995) Role of B61, the ligand for the Eck receptor tyrosine kinase, in TNF-α-induced angiogenesis, *Science 268*, 567–569.
33. Holmberg, J., Clarke, D. L., and Frisen, J. (2000) Regulation of repulsion versus adhesion by different splice forms of an Eph receptor, *Nature 408*, 203–206.
34. Ciossek, T., Millauer, B., and Ullrich, A. (1995) Identification of alternatively spliced mrnas encoding variants of MDK1, a novel receptor tyrosine kinase expressed in the murine nervous system, *Oncogene 10*, 97–108.
35. Valenzuela, D. M., *et al.* (1995) Identification of full-length and truncated forms of Ehk-3a novel member of the Eph receptor tyrosine kinase family, *Oncogene 10*, 1573–1580.
36. de Felipe, P., and Izquierdo, M. (2000) Tricistronic and tetracistronic retroviral vectors for gene transfer, *Hum. Gene Ther. 11*, 1921–1931.
37. de Felipe, P., Martin, V., Cortes, M., Ryan, M., and Izquierdo, M. (1999) Use of the 2A sequence from foot-and-mouth disease virus in the generation of retroviral vectors for gene therapy, *Gene Ther. 6*, 198–208.
38. de Felipe, P., and Ryan, M. (2004) Targeting of proteins derived from self-processing polyproteins containing multiple signal sequences, *Traffic 5*, 616–626.
39. Fotos, J. S., Patel, V. P., Karin, N. J., Temburni, M. K., Koh, J. T., and Galileo, D. S. (2006) Automated time-lapse microscopy and high-resolution tracking of cell migration, *Cytotechnology 51*, 7–19.